Consistency of global satellite-derived aerosol and cloud data sets with recent brightening observations

Jan Cermak,[1] Martin Wild,[1] Reto Knutti,[1] Michael I. Mishchenko,[2] and Andrew K. Heidinger[3]

Received 13 July 2010; revised 13 July 2010; accepted 23 August 2010; published 5 November 2010.

[1] Solar radiation at the Earth surface has increased over land and ocean since about 1990 ('global brightening'). An analysis of various global (ocean only) aerosol and (global) cloud data sets from geostationary and polar orbiting satellites is performed to determine whether changes in these quantities have occurred in accordance with 'global brightening', and to analyse the global distribution of these changes. Change-point detection and trend analysis are employed in the analysis. In a period from the mid-1980s to the mid-2000s, aerosol optical depth is found to have started declining in the early 1990s, while cloud data sets do not agree on trends. Ångström exponent data seem to suggest changes in pollution. **Citation:** Cermak, J., M. Wild, R. Knutti, M. I. Mishchenko, and A. K. Heidinger (2010), Consistency of global satellite-derived aerosol and cloud data sets with recent brightening observations, *Geophys. Res. Lett.*, *37*, L21704, doi:10.1029/2010GL044632.

1. Motivation and Aim

[2] Changes in solar radiation received at the Earth surface have been observed in many locations around the world, as well as in regional and global averages of surface solar radiation data. A negative trend in incoming radiation until about 1990 has been termed 'global dimming', whereas subsequent positive trends are referred to as 'global brightening' [*Stanhill and Cohen*, 2001; *Wild*, 2009]. Complementing station measurements over land, brightening trends have also been observed over ocean in satellite data [e.g., *Pinker et al.*, 2005; *Hinkelman et al.*, 2009].

[3] Changes in aerosol load and cloud cover are commonly identified as the main drivers of global dimming and brightening [*Streets et al.*, 2009; *Ruckstuhl et al.*, 2008]. *Mishchenko et al.* [2007] traced global brightening in satellite-derived global mean aerosol optical depth (AOD) data. *Mishchenko and Geogdzhayev* [2007] computed the differences between two three-year periods in the late 1980s and early 2000s to identify a general direction of change in AOD. However, they did not analyze whether these changes represented statistically significant trends, or when changes occurred. Indeed, no specific analysis relating global brightening to the global distribution and timing of significant aerosol and cloud trends and changes therein has been performed so far. It is therefore still unclear if trends in these two quantities are consistent with global brightening, and whether it can be attributed to anthropogenic changes in aerosol emissions.

[4] Global brightening is commonly assumed to have started in the 1980s to 1990s, which falls into the period of satellite observations. The aim of the study presented here is to evaluate global satellite-retrieved aerosol and cloud data sets to produce global maps of the distribution and onset of global brightening. From these temporal and spatial patterns conclusions can be drawn regarding the distribution and mechanisms of global brightening.

[5] The guiding hypotheses are:

[6] 1. Changes in aerosol and cloud distribution are responsible for the 'global brightening' phenomenon; global aerosol/cloud amount has started decreasing in the period for which satellite observations are available.

[7] 2. These changes are related to changes in human emission patterns; decreases should be observed when there are emission reductions (and vice versa).

2. Data and Methods

2.1. Data Sets

[8] The analysis performed here builds on global data sets derived from satellite-based observations. Ideally, an analysis of the relationships between aerosol and radiation trends should consider changes in single-scattering albedo. However, no long-term global data sets of this parameter exist. Instead, aerosol optical depth is chosen as a proxy for the total atmospheric aerosol load.

[9] For cloud amount information, the ISCCP monthly D2 product was used [*Rossow and Schiffer*, 1999] (1984–2005). It is based on data from the Advanced Very High Resolution Radiometer (AVHRR) and various geostationary satellite systems. Since long time series of this product may contain biases in some parts of the globe [*Evan et al.*, 2007], the Pathfinder Atmosphere extended (PATMOS-x) data set [*Heidinger and Pavolonis*, 2009] was used in addition (version 4 level 3). This data set is based on AVHRR observations only; afternoon observations were used, as only those are available continuously. PATMOS-x cloud fraction was used, as well as AOD at 0.63 μm [cf. *Zhao et al.*, 2008]. PATMOS-x covers the period from 1982–2007. For comparison, AOD was also used from the Global Aerosol Climatology Project (GACP) [*Mishchenko et al.*, 2007], from 1982–2005 (AOD at 0.55 μm). Like PATMOS-x the GACP product is based on AVHRR, but uses a different algorithm (differences outlined by *Zhao et al.* [2008]) and completely different radiance calibration procedures, which

[1]Institute for Atmospheric and Climate Science, ETH Zurich, Zurich, Switzerland.
[2]NASA Goddard Institute for Space Studies, New York, New York, USA.
[3]NOAA/NESDIS Center for Satellite Applications and Research, Madison, Wisconsin, USA.

0094-8276/10/2010GL044632

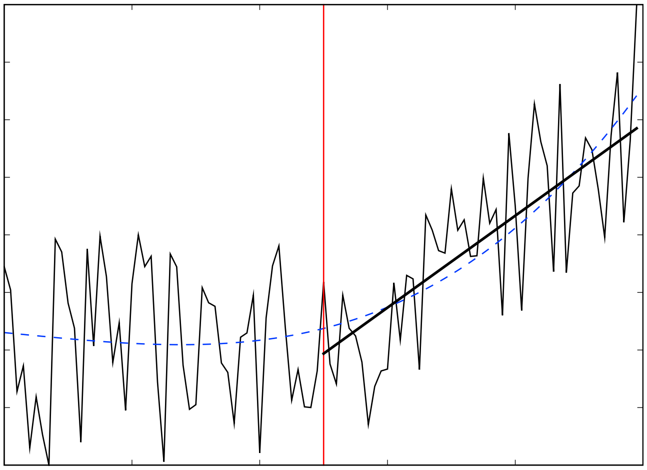

Figure 1. A synthetic time series (black solid) with cubic fit (blue dashed), change point (red solid, vertical) and trend (thick black solid).

increases the robustness of the trends on which both data sets agree. The GACP Ångström exponent data retrieved with AOD in a two-channel approach [*Mishchenko et al.*, 1999] were also included in the analysis. Both AOD products are available only over ocean.

[10] All data sets were available at spatial resolutions between 1° and 2.5° and at monthly intervals. As most data sets used are under ongoing development, the respective algorithms may sometimes produce erroneous results. Therefore all data points more than 2 standard deviations from the mean of each data set were removed. To avoid the masking of long-term trends by short-term changes in the aerosol time series stemming from the eruptions of El Chichón (April 1982) and Mt. Pinatubo (June 1991), data for the remainder of the eruption year plus the following two (Chichon) or three (Pinatubo) years were removed from the aerosol data sets. The PATMOS-x cloud algorithm quality suffered from a channel shift on the AVHRR instrument from January 2001 to April 2003. These data were removed as well.

[11] The interpretation of trends and regional patterns can sometimes be impeded by artefacts stemming from satellite system transitions and combinations [*Evan et al.*, 2007]. The data sets used in this study are products of careful efforts at harmonizing time series; they have been filtered for this study, and known limitations are addressed where appropriate.

2.2. Identification of Trend Changes

[12] The concept of change point detection was used to determine the onset of brightening trends in the various data sets. In this approach, data series are analysed statistically to find discontinuities in the trends contained therein (cf. *Peterson et al.* [1998] for a review). In general these techniques identify data series changes by evaluating a metric computed for the environment of each data point (moving window approach). For the purpose of this study, change points were found by minimizing

$$S = \frac{\min(p(t_l), p(t_r))}{abs(s(t_l) - s(t_r)) \times e(t_{l+r})} \quad (1)$$

with S a change point score, p the probability of a trend t being insignificant, s its slope, e the trend fitting error, t_l the trend of the subseries to the left of a point being tested, t_r to the right and t_{l+r} the trend of the combined subseries. This procedure aims to find a point at which at least one highly significant trend starts or ends ($\min(p(t_l),p(t_r))$), while the significance of the trend passing through this point is as low as possible (high $e(t_{l+r})$) and the difference in slopes on both sides of the potential change point ($abs(s(t_l) - s(t_r))$) is maximized. The subseries on the right and left are of equal length.

[13] S is computed for each point in the cubic fit to the data series; the change point is identified where S is at its minimum. A time series with change point is shown in Figure 1.

[14] The performance of this technique was tested on time series with 'known' change points with random noise added. 100 of these series represented the reversal of a trend, another 100 a transition from no trend to a significant trend. On these time series, the mean error in change point detection was between 0.5 and 1%, with a standard deviation between 2 and 5%. Other methods also tested yielded considerably less reliable results. In particular, methods searching for a minimum/maximum of a fitted curve fail in cases where part of the time series shows a near-zero trend (e.g., left half of Figure 1).

[15] The specific purpose of this study is to identify the onset of trends within the time series considered. Therefore, the subseries remaining between a change point and the end of the data series was tested for significant linear trends (95% level) spanning at least 75% of this interval. Where no such trend was found, the change point was discarded and the total series tested for trends spanning at least 75% of the total data series and significant at the 95% level.

[16] Each data series was thus categorized as one of the following: (1) Change point followed by positive trend, (2) change point followed by negative trend, (3) no change point, positive overall trend, (4) no change point, negative overall trend, (5) no change point, no overall trend. Evaluation of change points and trends was performed for regions of 15 × 15° in each data set as well as for global, hemispheric, ocean and land means.

3. Results and Discussion

3.1. Spatial Patterns of Change

[17] Figure 2 shows the results of the categorization described above for aerosol and cloud parameters respectively.

[18] PATMOS-x and GACP show a general decline in AOD on both hemispheres. In the PATMOS-x data set almost all 15° boxes show turns to negative trends. In this map, some positive overall trends are found, e.g. near India, Indonesia and in the Beijing Bay (only a small red patch, because there is not much ocean area in this box). In the GACP data set many boxes, particularly in the Northern hemisphere, show overall negative trends, indicating that a decline in AOD persisted. Some of these long trends are found near North America and Europe, where they would appear to be consistent with presumed very early onsets of brightening.

[19] Generally, most change points are in the range from 1991 to 1995, with GACP reporting changes earlier than

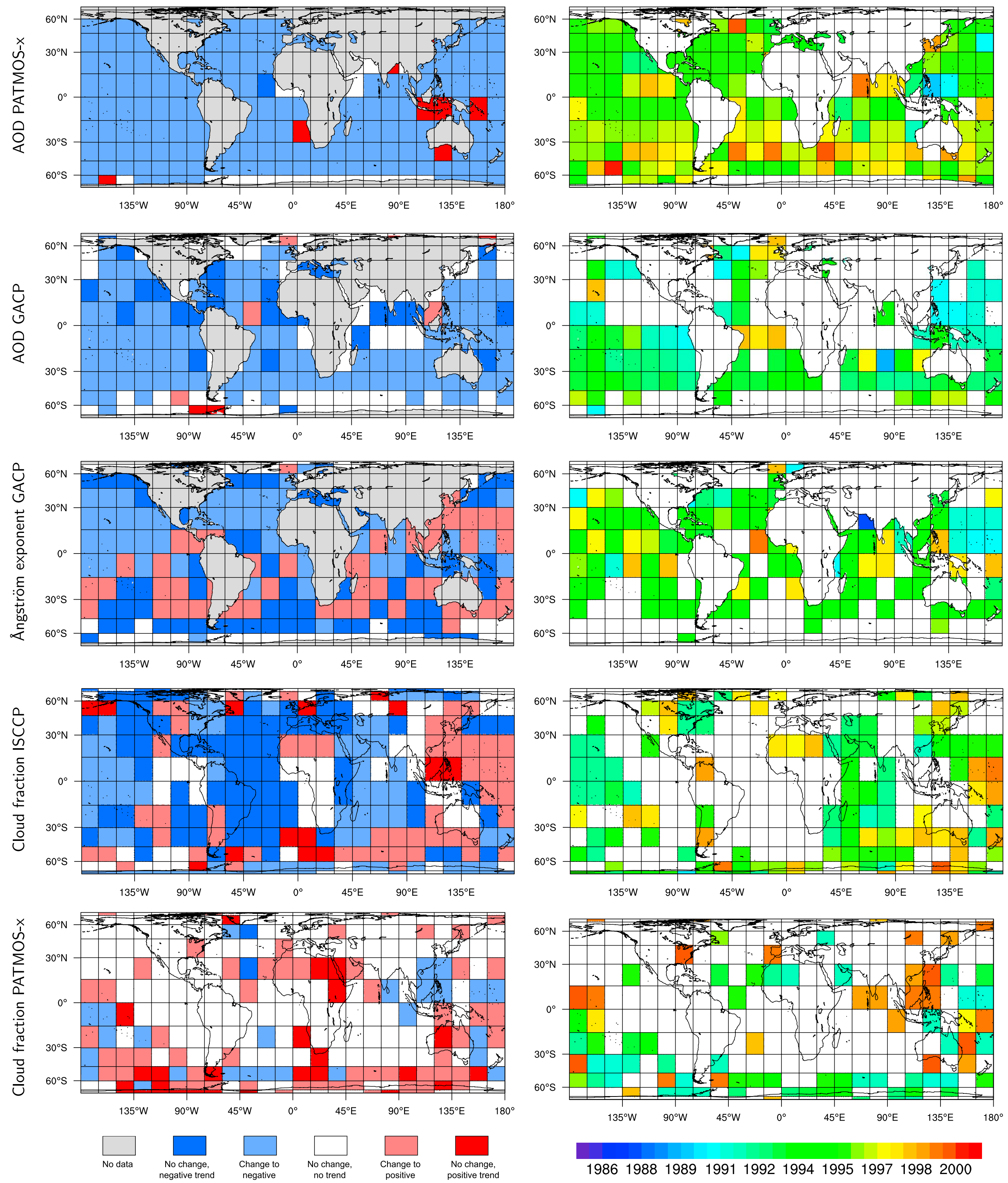

Figure 2. Changes and trends in the data sets. (left) Trends and change points for each data set (details see text); (right) year of trend change. NB: Aerosol data sets only cover the oceans.

PATMOS-x. Most of these points fall in the period blanked out in the original data series due to the Pinatubo eruption. It is therefore impossible to decide when exactly the trends changed. However, the good agreement between both data sets strongly suggests that changes did occur and that negative trends began during this period. In both data sets, trend changes in the southern hemisphere lag those in the north.

[20] The overall negative trends observed in the GACP data set appear more credible for these particular locations. The AOD values after the Pinatubo gap (start of negative trend) in PATMOS-x are clearly above the pre-Pinatubo level, whereas in GACP they are at roughly the same level.

[21] Changes in the GACP Ångström exponent differ between hemispheres. While in the north, changes to neg-

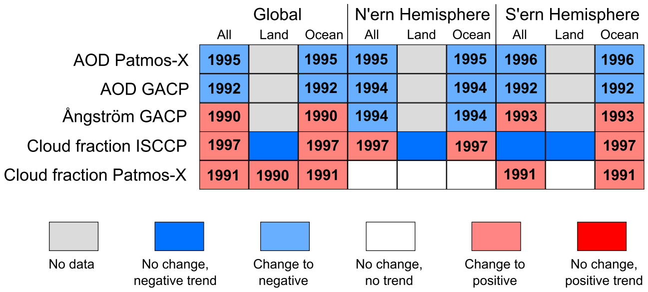

Figure 3. Trends and changes in all parameter on various spatial scales. Numbers in the cells indicate the years the respective changes occurred. Aerosol data sets cover ocean only ('All' equals 'Ocean').

ative trends prevail, the southern hemisphere displays many changes to positive trends. In the high latitudes, overall negative trends dominate on both sides. Most changes occurred in the early 1990s.

[22] The turn to negative Ångström exponent trends in the northern hemisphere could be an indication of reduced anthropogenic emissions and thus a smaller aerosol fine mode fraction. Positive turns encountered in the south indicate rising fine mode fractions (in accordance with *Stern* [2006]). These could be due to increased winds leading to higher concentrations of atmospheric sea salt aerosol (as suggested by *Mishchenko and Geogdzhayev* [2007]). However, while these interpretations would be in accordance with the expected patterns, the observed changes in Ångström exponent could also be impacted by multi-modal aerosol distributions or non-spherical particles [*Schuster et al.*, 2006; *Mishchenko et al.*, 2003].

[23] The last two rows in Figure 2 summarize changes found in the cloud data sets. The ISCCP cloud fraction indicates large areas with negative trends throughout the time period considered. In the Indian and central Pacific oceans, areas with turns to negative trends are visible, with turning points in the first half of the 1990s. In some regions, notably some parts of North America, Eastern Asia, the western Pacific and northern Africa, positive trends begin in the second half of the 1990s.

[24] As shown by *Evan et al.* [2007], there is a systematic negative trend in ISCCP total cloud amounts from 1985 to 2000 that is not seen in other cloud amount data sets. This trend is driven by regions at the coverage edges of the geostationary satellites used in the data set. This irregularity may be reflected in Figure 2.

[25] The PATMOS-x cloud fraction data set appears to disagree with the ISCCP observations. Most of the 15 by 15 degree boxes do not show any trend at all, and the majority of the changes observed appear to point in a positive direction (in contrast to the ISCCP overall picture).

3.2. Global Summary

[26] The analysis performed for 15 degree boxes above was also performed on global mean, hemispheric mean, as well as land and ocean mean data series. The results are shown in Figure 3. These figures represent a global picture of the tendencies analysed above. However, apparent disagreement with the above analysis, in particular regarding turning point years is possible in some cases, because the mean time series used here include areas with no trends or trends in opposing directions.

[27] The aerosol optical depth recedes in both GACP and PATMOS-x data sets from the first half of the 1990s. The GACP Ångström exponent turns to positive globally and in the southern hemisphere, and to negative in the northern hemisphere.

[28] Disagreements in cloud fraction trends are pronounced; changes to positive trends, where present, occur earlier in PATMOS-x than in ISCCP global cloud fraction.

4. Conclusions

[29] The aim of this study was to determine whether changes in aerosol cloud occurrence and are consistent with 'global brightening' observations. The patterns found seem to concur with expectations in principle.

[30] The analysis contains several uncertainties. Some of these relate to the data used: All data sets potentially contain inconsistencies caused by sensor changes during the period considered here; also, gaps in the data series were caused by the filtering outlined above. While all data sets used relied on different satellite retrieval algorithms, they are mostly based on the same sensors (AVHRR, albeit with independent radiance calibration procedures); given that AVHRR data is one of the longest satellite time series, this can hardly be avoided in climatological analyses today. Also, more sophisticated, newer systems would be able to provide additional parameters, such as single-scattering albedo, which are absent in the data sets used here. The methodology of change point detection might produce errors in addition to the shortcomings of the data sets, such as misattribution or miss of change points. Likewise, change points at or beyond the ends of the time series will not be detected here.

[31] Bearing these limitations in mind, the overall picture revealed in this study still seems to be of a certain robustness, at least for aerosol. Both AOD data sets agree that negative trends started in the period considered here, with some regions possibly displaying negative trends throughout. These trends started in the early 1990s, with the southern hemisphere slightly lagging the northern hemisphere. Some positive trends in southern and south-east Asia seem to concur with industrial development in these regions.

[32] This is also supported by the results of the Ångström exponent analysis. Observed changes seem to agree with expectations in that a decrease is found in most of the northern hemisphere (less fine-mode pollution) and increase in east Asia and the southern hemisphere (more pollution) [cf. *Akimoto*, 2003]. Predominantly latitudinal aerosol transport means that anthropogenic emission changes also register over the oceans, possibly with a delay.

[33] Concerning the initial hypotheses, it thus seems that trends in AOD as given in the data sets considered support global brightening observations, whereas cloud observations are inconclusive. The large differences in the cloud data sets may either be due to inconsistencies in the data sets (cf. *Evan et al.* [2007] for ISCCP) or to error margins exceeding the variation in the data. An aerosol-size-centered interpretation of Ångström exponent patterns would support the second hypothesis, i.e. that human emission patterns have changed.

[34] In summary, this study for the first time provides insights into the timing and spatial distribution of changes in aerosol trends related to global brightening based on satellite observations. This was possible on the basis of change-point detection analysis coupled with tests of statistical trend significance.

[35] **Acknowledgments.** The comments and suggestions of two anonymous reviewers helped improve this paper. The views, opinions, and findings contained in this report are those of the authors and should not be construed as an official NOAA or U.S. Government position, policy, or decision.

References

Akimoto, H. (2003), Global air quality and pollution, *Science*, *302*(5651), 1716–1719, doi:10.1126/science.1092666.

Evan, A. T., A. K. Heidinger, and D. J. Vimont (2007), Arguments against a physical long-term trend in global ISCCP cloud amounts, *Geophys. Res. Lett.*, *34*, L04701, doi:10.1029/2006GL028083.

Heidinger, A. K., and M. J. Pavolonis (2009), Gazing at cirrus clouds for 25 years through a split window. Part I: Methodology, *J. Appl. Meteorol. Climatol.*, *48*(6), 1100–1116, doi:10.1175/2008JAMC1882.1.

Hinkelman, L. M., P. W. Stackhouse, B. A. Wielicki, T. Zhang, and S. R. Wilson (2009), Surface insolation trends from satellite and ground measurements: Comparisons and challenges, *J. Geophys. Res.*, *114*, D00D20, doi:10.1029/2008JD011004.

Mishchenko, M. I., and I. V. Geogdzhayev (2007), Satellite remote sensing reveals regional tropospheric aerosol trends, *Opt. Express*, *15*(12), 7423–7438, doi:10.1364/OE.15.007423.

Mishchenko, M., I. Geogdzhayev, B. Cairns, W. Rossow, and A. Lacis (1999), Aerosol retrievals over the ocean using channel 1 and 2 AVHRR data: A sensitivity analysis and preliminary results, *Appl. Opt.*, *38*, 7325–7341, doi:10.1364/AO.38.007325.

Mishchenko, M. I., I. V. Geogdzhayev, L. Liu, J. A. Ogren, A. A. Lacis, W. B. Rossow, J. W. Hovenier, H. Volten, and O. Muñoz (2003), Aerosol retrievals from AVHRR radiances: Effects of particle nonsphericity and absorption and an updated long-term global climatology of aerosol properties, *J. Quant. Spectrosc. Radiat. Transfer*, *79–80*, 953–972, doi:10.1016/S0022-4073(02)00331-X.

Mishchenko, M. I., I. V. Geogdzhayev, W. B. Rossow, B. Cairns, B. E. Carlson, A. A. Lacis, L. Liu, and L. D. Travis (2007), Long-term satellite record reveals likely recent aerosol trend, *Science*, *315*(5818), 1543, doi:10.1126/science.1136709.

Peterson, T. C., et al. (1998), Homogeneity adjustments of in situ atmospheric climate data: a review, *Int. J. Climatol.*, *18*(13), 1493–1517, doi:10.1002/(SICI)1097-0088(19981115)18:13<1493::AID-JOC329>3.0.CO;2-T.

Pinker, R. T., B. Zhang, and E. G. Dutton (2005), Do satellites detect trends in surface solar radiation?, *Science*, *308*(5723), 850–854, doi:10.1126/science.1103159.

Rossow, W., and R. Schiffer (1999), Advances in understanding clouds from ISCCP, *Bull. Am. Meteorol. Soc.*, *80*, 2261–2287, doi:10.1175/1520-0477(1999)080<2261:AIUCFI>2.0.CO;2.

Ruckstuhl, C., et al. (2008), Aerosol and cloud effects on solar brightening and the recent rapid warming, *Geophys. Res. Lett.*, *35*, L12708, doi:10.1029/2008GL034228.

Schuster, G. L., O. Dubovik, and B. N. Holben (2006), Angstrom exponent and bimodal aerosol size distributions, *J. Geophys. Res.*, *111*, D07207, doi:10.1029/2005JD006328.

Stanhill, G., and S. Cohen (2001), Global dimming: A review of the evidence for a widespread and significant reduction in global radiation with discussion of its probable causes and possible agricultural consequences, *Agric. For. Meteorol.*, *107*(4), 255–278, doi:10.1016/S0168-1923(00)00241-0.

Stern, D. I. (2006), Reversal of the trend in global anthropogenic sulfur emissions, *Global Environ. Change*, *16*(2), 207–220, doi:10.1016/j.gloenvcha.2006.01.001.

Streets, D. G., F. Yan, M. Chin, T. Diehl, N. Mahowald, M. Schultz, M. Wild, Y. Wu, and C. Yu (2009), Anthropogenic and natural contributions to regional trends in aerosol optical depth, 1980–2006, *J. Geophys. Res.*, *114*, D00D18, doi:10.1029/2008JD011624.

Wild, M. (2009), Global dimming and brightening: A review, *J. Geophys. Res.*, *114*, D00D16, doi:10.1029/2008JD011470.

Zhao, T. X. P., I. Laszlo, W. Guo, A. Heidinger, C. Cao, A. Jelenak, D. Tarpley, and J. Sullivan (2008), Study of long-term trend in aerosol optical thickness observed from operational AVHRR satellite instrument, *J. Geophys. Res.*, *113*, D07201, doi:10.1029/2007JD009061.

J. Cermak, M. Wild, and R. Knutti, Institute for Atmospheric and Climate Science, ETH Zurich, Universitätstr. 16, CH-8092 Zurich, Switzerland. (jan.cermak@env.ethz.ch)

M. I. Mishchenko, NASA Goddard Institute for Space Studies, 2880 Broadway, New York, NY 10025, USA.

A. K. Heidinger, NOAA/NESDIS Center for Satellite Applications and Research (STAR), 1225 West Dayton, Madison, WI 53706, USA.